



**PAPER**

## Comparative study of crystallite size using Williamson-Hall and Debye-Scherrer plots for ZnO nanoparticles

To cite this article: S Mustapha *et al* 2019 *Adv. Nat. Sci: Nanosci. Nanotechnol.* **10** 045013

View the [article online](#) for updates and enhancements.

# Comparative study of crystallite size using Williamson-Hall and Debye-Scherrer plots for ZnO nanoparticles

S Mustapha<sup>1,2</sup>, M M Ndamitso<sup>1,3</sup>, A S Abdulkareem<sup>2,3</sup>, J O Tijani<sup>1,3</sup>,  
D T Shuaib<sup>4</sup>, A K Mohammed<sup>5</sup> and A Sumaila<sup>6</sup>

<sup>1</sup> Department of Chemistry, Federal University of Technology, PMB 65, Bosso Campus, Minna, Nigeria

<sup>2</sup> Nanotechnology Research Group, Center for Genetic Engineering and Biotechnology, Federal University of Technology, Minna, PMB 65, Niger State, Nigeria

<sup>3</sup> Department of Chemical Engineering, Federal University of Technology, PMB 65, Gidan Kwano Campus, Minna, Niger State, Nigeria

<sup>4</sup> Department of Chemistry, Illinois Institute of Technology, 3101 S Dearborn Street, Chicago, IL 60616 United States of America

<sup>5</sup> Department of Chemistry and Biochemistry, North Carolina Central University, 1801 Fayetteville Street, Durham, North Carolina 27707 United States of America

<sup>6</sup> Department of Pure and Industrial Chemistry, Anyigba, Kogi State, Nigeria

E-mail: [saheedmustapha09@gmail.com](mailto:saheedmustapha09@gmail.com)

Received 9 August 2019

Accepted for publication 3 October 2019

Published 14 November 2019



CrossMark

## Abstract

ZnO nanoparticles at different pH were synthesised by a sol-gel technique from zinc acetate dihydrate at a calcination temperature of 450 °C. The synthesized ZnO nanoparticles were characterised by x-ray diffraction (XRD) peak profile analysis, high-resolution scanning electron microscopy and Fourier transform infrared spectroscopy. The effects of solution pH on the crystallite size using Williamson-Hall and Debye-Scherrer were determined. The XRD analysis of the zincite phase structure of ZnO nanoparticles was obtained in the form of spheres for all the samples. The average crystallite sizes of ZnO nanoparticles decrease with increasing pH. The crystallite sizes of ZnO nanoparticles were investigated using Williamson-Hall analysis and Scherrer's formula. The parameters such as dislocation density and lattice strain were computed for the diffraction peaks of XRD in the range of  $2\theta = 10-90^\circ$ . The results showed that the crystallite sizes calculated from Scherrer's equation and Williamson-Hall analysis from XRD are not inter-correlated. Both methods give a wide deviation of crystallite size. Also, it was found that the crystallite sizes using both methods decrease with an increase in pH. Smaller crystallite sizes were estimated using the Scherrer's formula. Thus, it is deduced that the equation fitted well for the synthesised ZnO nanoparticles.

Keywords: ZnO nanoparticles, characterised, crystallite sizes, Williamson-Hall analysis, Scherrer's formula

Classification numbers: 2.00, 4.02, 4.03

## 1. Introduction

Zinc oxide (ZnO) is a non-toxic, semiconductor material which has been widely studied in the past years as a result of its fundamental and attractive characteristics. Its technological importance includes a wide band gap, good chemical stability, suitable electrical and optical properties as reported by many

researchers. Crystal morphology and particle size play vital roles in the application, which have led scholars to focus on the synthesis of ZnO nanoparticles. Both physical and chemical methods have been employed for the synthesis of ZnO nanoparticles such as sol-gel [1], thermal plasma synthesis [2], hydrothermal synthesis [3], spray pyrolysis [4], chemical precipitation [5], combustion synthesis [6], electrochemical

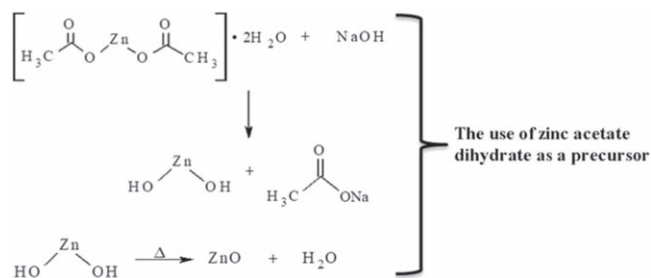


**Figure 1.** Hydrolysis and condensation reactions of acetate dihydrate for ZnO.

route [7] and among others. Extensive literature evaluation concludes that sol-gel is the commonly selected method for the synthesis of ZnO nanoparticles. This is because this method produces excellent crystalline structure and narrow size distribution. This method requires low-temperature, easy composition control and low cost-effectiveness.

Besides the synthesis procedures, parameters including temperature, pH of the solution, ageing time, stirring time, the concentration of the precursors and type of solvent used plays important role in nucleation and growth of ZnO nanoparticles. Serious attention has been given to the synthesis and characterisation of nanoparticles, but only a few articles have been published on the effect of pH variation on crystal size of ZnO nanoparticles synthesised by sol-gel technique.

For instance, Parra and Haque [8] synthesised ZnO powder by sol-gel route without using capping agents such as PEG, PAM and among others.  $Zn(CH_3COO)_2 \cdot 2H_2O$  was dissolved in distilled water and NaOH which serves as precipitating agent and pH controller was subsequently added to the solution to maintain a pH of 8. During the process, a white precipitate was formed which was washed with de-ionised water and ethanol. After 3 h, a milky white colour ZnO nanoparticle powder was obtained at different temperatures of 200, 400 and 500 °C for 3 h. The similar investigation was conducted by Ashraf *et al* [9] on the structural and optical properties of ZnO nanoparticles. Bhardwaj *et al* [10] synthesised ZnO nanoparticles using  $Zn(CH_3COO)_2 \cdot 2H_2O$  and KOH by sol-gel route. The solution was stirred to form a milky precipitate which was centrifuged at 3000 rpm and then dried at 80 °C for 6 h. In their findings, the ZnO spherical nanoparticle structure was formed. The report of Manikandan *et al* [11] on the synthesised ZnO nanoparticles by sol-gel technique showed that the nanoparticles were prepared at a pH of 8 using NaOH as pH adjuster. Zinc acetate was added to ethanol and then stirred for 1 h. NaOH was added to the solution and further stirred for 3 h to obtain the homogeneous gel. The gel was oven dried at 60 °C and allowed to age overnight. It was then washed with distilled water and ethanol. Finally, the dried gel was calcined at 500 °C for 4 h to obtain ZnO nanoparticles. Acosta-Humanez *et al* [12] prepared ZnO by sol-gel method using  $Zn(NO_3)_2 \cdot 6H_2O$  as the pioneering material and citric acid ( $C_6H_8O_7 \cdot H_2O$ ) as a complexing agent effective at 70 °C with vigorous stirring until

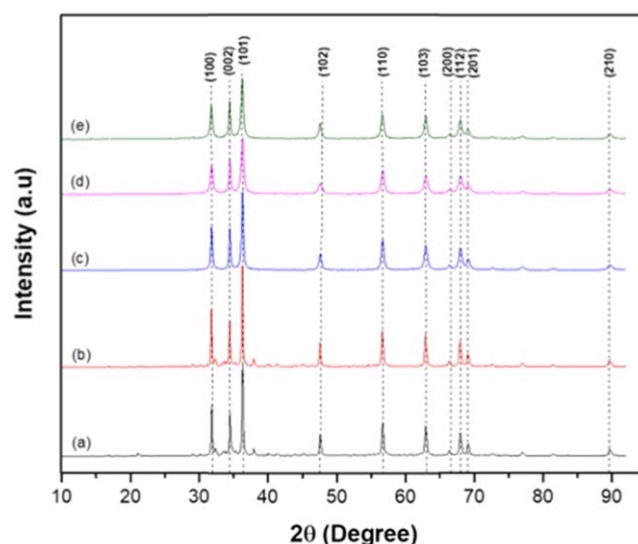


**Figure 2.** XRD patterns for ZnO prepared at pH (a) 4, (b) 6, (c) 8, (d) 10 and (e) 12 calcined at 450 °C.

the gel was formed. Calcination was done for 12 h at 130 °C. It was confirmed that the ZnO nanoparticles (wurtzite structure) were dominant. Mohan and Renjanadevi [13] synthesised ZnO using  $ZnSO_4 \cdot 7H_2O$  as precursor and NaOH as a precipitating agent and stirred for several hours. The white precipitate was filtered and washed with distilled water, calcined at 100 °C and then ground to form fine powders. ZnO nanoparticles formed showed a noticeable colour change from white to a dark ash colour. The as-prepared ZnO powder was calcined at a temperature ranging from 500 to 900 °C at 200 °C interval. Akkari *et al* [14] prepared ZnO nanoparticles by dissolving zinc acetate in methanol with KOH methanol under vigorous stirring. The resulting precipitate was washed with ethanol. Prior to the authors' experimental design, the generated colloidal ZnO nanoparticles were sealed in a container and kept for further use.

The quantitative analysis determined the phase composition, lattice parameter, crystalline size and degree of crystallinity of nanomaterials. Some of the methods used for quantitative analysis were Scherrer's equation, Williamson-Hall method, Warren-Averbach analysis, Rietveld refinement and pseudo-Voigt function [15]. However, Williamson-Hall (W-H) analysis for crystallite size and strain analysis is still under-utilised when compared to the Scherrer's equation. Among the various techniques used for the measure of crystallite sizes, x-ray diffractometer (XRD) remains a dominant method for crystallite size determination. The other major feature extracted from peak width XRD analysis is lattice strain. Crystalline size and lattice strain measure the size of coherently diffracting domains and the distribution of lattice constants from lattice dislocations, respectively.

In this study, a sol-gel technique was used to synthesise ZnO nanoparticles. The prepared samples were characterised by x-ray diffraction (XRD), high-resolution scanning electron microscope (HRSEM), high-resolution transmission electron

**Table 1.** Average crystallite size of ZnO at different pH for the Scherrer’s formula and the W-H analysis.

Parameter	pH					
	4	6	8	10	12	
Phase		Zincite	Zincite	Zincite	Zincite	Zincite
Scherrer	$D$ (nm)	22.58	24.82	16.10	11.84	14.10
	$\delta$ ( $\text{nm}^{-2}$ )	0.20	0.16	0.39	0.71	0.50
Williamson-Hall	$D$ (nm)	61.70	75.52	46.77	28.32	29.71
	$\delta$ ( $\text{nm}^{-2}$ )	0.26	0.18	0.46	1.30	1.10
	$\epsilon \times 10^{-2}$	8.82	7.26	13.84	23.73	11.88
Lattice parameter	$a$ (Å)	3.25	3.25	3.25	3.25	3.25
	$c$ (Å)	5.21	5.21	5.21	5.21	5.21
	$a/c$	0.62	0.62	0.62	0.62	0.62
Lattice structure		Hexagonal	Hexagonal	Hexagonal	Hexagonal	Hexagonal

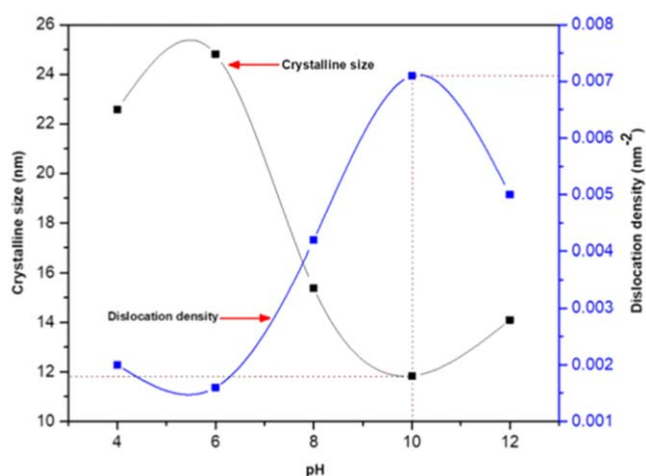


**Figure 3.** Plot of crystalline size and dislocation against pH of ZnO nanoparticles using Debye-Scherrer analysis.

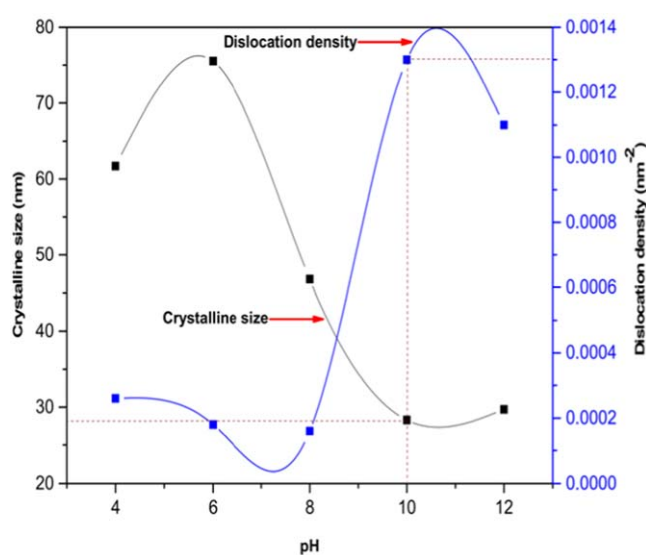


**Figure 4.** Plot of crystalline size and dislocation against pH of ZnO nanoparticles using W-H analysis.

microscope (HRTEM) and Fourier transform infra-red (FTIR). In addition, a comparative evaluation of crystallite size XRD analysis using Scherrer’s equation and W-H analysis is reported.

## 2. Materials and methods

### 2.1. Zinc oxide nanoparticles via sol-gel method

The zinc oxide nanoparticles were synthesised using a modified sol-gel method. 50 cm<sup>3</sup> of zinc acetate dihydrate [Zn(C<sub>2</sub>H<sub>3</sub>O<sub>2</sub>)<sub>2</sub>·2H<sub>2</sub>O] solution was measured into a 250 cm<sup>3</sup> beaker and about 100 cm<sup>3</sup> of de-ionised water was added. The solution was stirred using a magnetic stirrer for 30 min at 150 rpm. 0.5 M sodium hydroxide (NaOH) was added dropwise to the solution to obtain the desired pH of 4, 6, 8, 10 and 12. The mixture was stirred for 5 min and the precipitate was obtained and later filtered by Whatmann No. 1 filter paper. The residue obtained was washed with deionised water and ethanol to eliminate traces of the unreacted precursors. The final product was oven dried at 105 °C for 24 h and finally

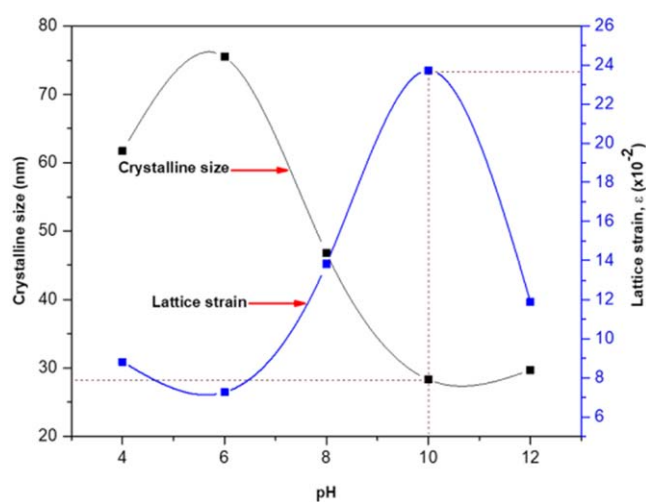


**Figure 5.** Plot of crystalline size and lattice strain against pH of ZnO nanoparticles using Williamson-Hall analysis.

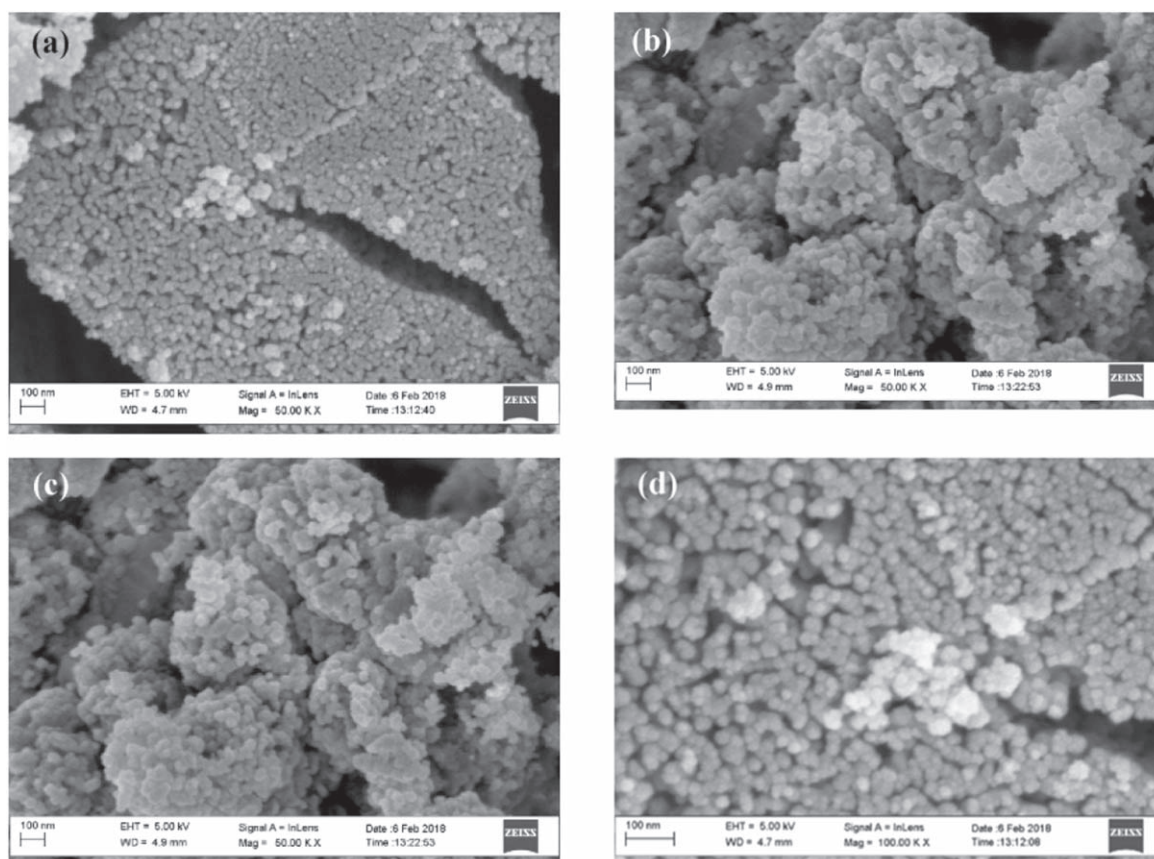


**Figure 6.** EDX analysis of ZnO nanoparticles in atomic percentage.

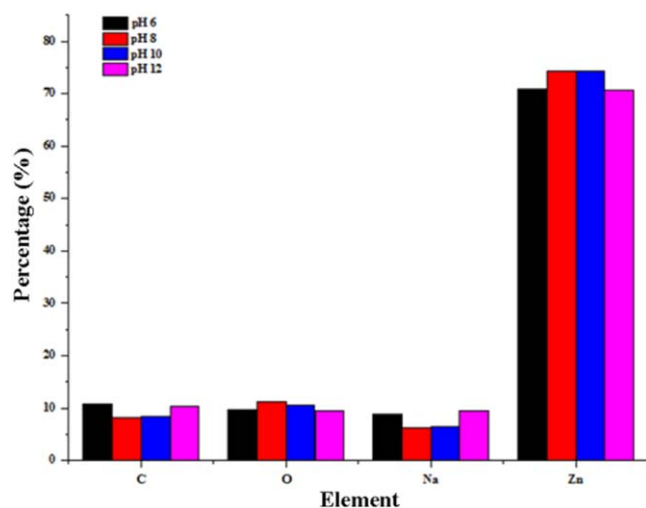


**Figure 7.** EDX spectra of ZnO nanoparticles at different pH values.

calcined in the furnace at a temperature of 450 °C to obtain ZnO nanoparticles.

## 2.2. Synthesis of ZnO

In the sol-gel technique, precursors often used are zinc acetate dihydrate, zinc nitrate hexahydrate, zinc chloride, zinc sulphate and zinc acetylacetonate. During this process, ageing

time, pH and temperature have effects on the synthesised nanoparticles. The morphology and shape of ZnO are controlled by solution pH of the synthesised sol. The amount of hydrogen and hydroxyl ions ( $H^+$  and  $OH^-$ ) in the synthesised sols plays a vital role to control morphology and grain size. The quantity of  $H^+$  and  $OH^-$  ions polymerised with the metal to oxygen bonds during the synthesis. Zinc hydroxide is produced in both steps and upon heating, ZnO nanoparticles are formed. This zinc hydroxide separates into  $Zn^{2+}$  and  $OH^-$ , followed by polymerisation of hydroxyl complex to yield Zn-O-Zn and finally converted into ZnO as shown in figure 1. Hence, the pH of the precursor solution affects hydrolysis and condensation of the sols.

## 2.3. Characterisations of ZnO nanoparticles

The crystal phase composition and the crystal size of the ZnO nanoparticles were determined using x-ray diffraction (Bruker AXS D8 Advance, x-ray diffractometer) with  $Cu-K\alpha$  radiation (1.5406 Å) in the range of  $2\theta = 10^\circ-90^\circ$ . The morphology and structure of the nanoparticles were investigated using high-resolution scanning electron microscopy (Auriga ZEISS) with energy-dispersive x-ray spectroscopy (EDX). The Fourier transform infrared (FTIR) spectra were recorded using the Thermo/Scientific, Nicolet iS5.

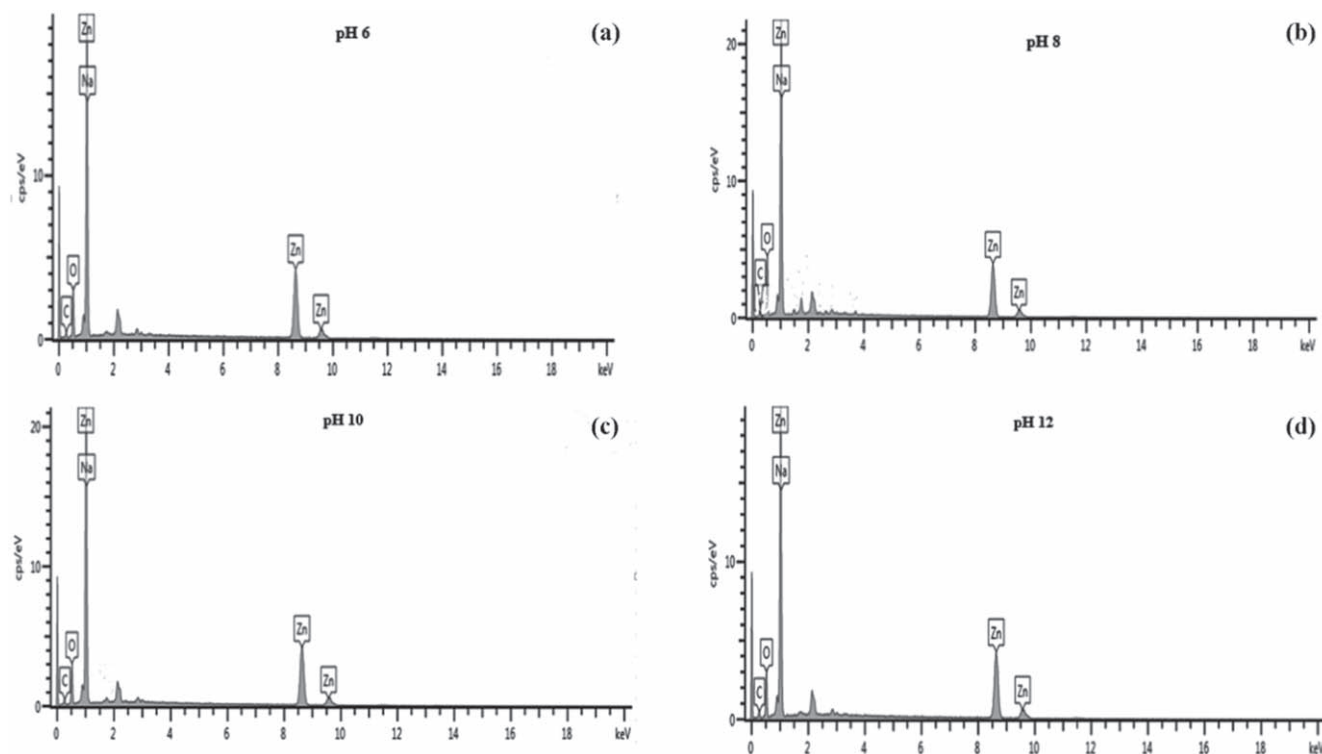


**Figure 8.** FTIR spectra of synthesized ZnO nanoparticles at pH (a) 6, (b) 8, (c) 10 and (d) 12 calcined at 450 °C.

**Table 2.** EDX results of ZnO nanoparticles at pH 6, 8, 10 and 12.

Element	pH							
	6		8		10		12	
	% wt	% at	% wt	% at	% wt	% at	% wt	% at
Carbon	8.08	24.01	10.80	30.30	8.42	25.00	10.28	29.05
Oxygen	11.19	25.00	9.64	20.20	10.59	23.57	9.58	20.27
Sodium	6.31	9.68	8.78	12.80	6.55	10.36	9.50	13.85
Zinc	74.42	41.22	70.78	36.70	74.43	41.07	70.64	36.82

### 3. Results and discussion

#### 3.1. XRD analysis

The XRD patterns for ZnO prepared at pH 4, 6, 8, 10 and 12 are shown in figure 2. In the study, the solubility of as-synthesised ZnO in acidic medium ( $\text{pH} < 7$ ) was high. This is because of the presence of a high and low concentration of  $\text{H}^+$  and  $\text{OH}^-$  in the sol respectively. At high pH (greater than 7) condition, the amount of  $\text{OH}^-$  from hydroxyl base reacting with  $\text{H}^+$  ions in the sol is higher. Thus, using alkali favoured the formation of ZnO. Result obtained shows diffraction peaks at  $31.77^\circ$ ,  $34.42^\circ$ ,  $36.25^\circ$ ,  $47.54^\circ$ ,  $56.60^\circ$ ,  $62.85^\circ$ ,  $66.38^\circ$ ,  $67.96^\circ$ ,  $69.10^\circ$  and  $89.61^\circ$  in the spectra at diffraction lines (110), (002), (101), (102), (110), (103), (200), (112), (203) and (201), respectively. The cell constants are  $a = b = 3.25 \text{ \AA}$ . These values are in accordance with the peaks of the standard card file JCPDS-00-036-1451 and are indexed as the hexagonal zincite structure.

The XRD patterns of the samples showed similar zincite peaks at almost the same diffraction angles as presented in figure 2. Crystallite sizes were calculated in comparison using Debye–Scherrer and Williamson–Hall equations as follows:

$$D = \frac{k\lambda}{\beta \cos \theta}, \quad (1)$$

where  $D$  is the crystallite size (nm),  $k$  is a constant (0.94 for spherical particles),  $\lambda$  is the wavelength of the x-ray radiation ( $\text{Cu-K}\alpha = 0.1541 \text{ nm}$ ),  $\beta$  is the full width at half maximum (FWHM) of the intense and broad peaks and  $\theta$  is the Bragg's or diffraction angle.

$$\beta \cos \theta = \frac{k\lambda}{D} + 4\varepsilon \sin \theta. \quad (2)$$

Crystalline sizes obtained at pH 4, 6, 8, 10 and 12 for ZnO nanoparticles calcined at 450 °C were achieved respectively from the aforementioned diffraction peaks.

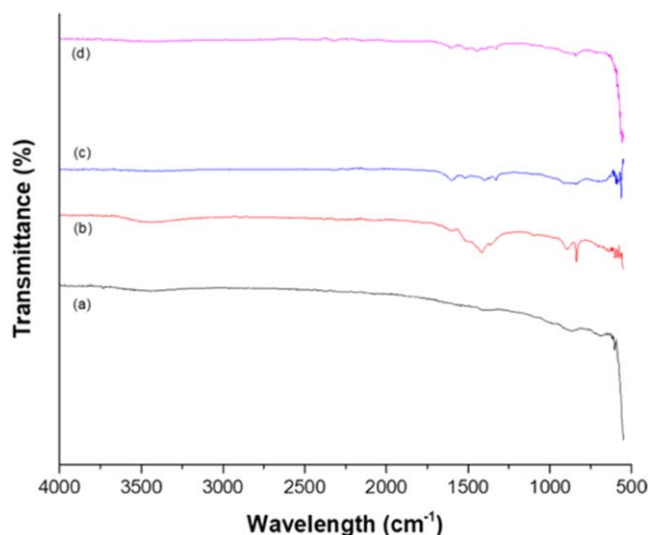


**Figure 9.** A Williamson-Hall plot of  $\beta \cos \theta$  against  $4 \sin \theta$  calculated from XRD diffractogram for ZnO nanoparticles at different pH calcined at 450 °C.

The dislocation density ( $\delta$ ) as shown in table 2 which indicates the deficiency in the nanoparticles was calculated using the formula:

$$\delta = \frac{1}{D^2}, \quad (3)$$

where the dislocation density is inversely proportional to the grain size/crystallite size of ZnO nanoparticles calculated from Scherrer's formula.

The observed highest peak intensity appearing at pH 6 and 8 is due to an adequate amount of  $\text{OH}^-$  to form ZnO. No other peaks of impurity or unreacted phase were formed for the ZnO samples at all levels of pH values, showing that the precursors were completely decomposed at the calcination temperature of 450 °C and no other products were formed. All the ZnO samples with diffraction lines (101), (002) and (101) are narrower than other diffraction lines. It was observed that as the pH became more basic, the diffraction lines were broadened, causing particles to become smaller. Thus, smaller nanoparticles are formed at high pH. The average crystallite size of 11.84 to 24.82 nm of as-prepared ZnO nanoparticles was calculated using the Scherrer's equation and other values of parameters such as wavelength and shape factor remain constant.

As shown in table 1, the results of the calculated crystallite size were summarised from Scherrer's and Williamson-Hall formulae using OriginPro 2015 software. Generally, the average particle size was larger at low pH but there is a decrease in crystal size at high pH. This could be as a result of fine particles of ZnO produced at high pH value and the augmentation in precursor-to-volume of sodium hydroxide ratio. The dislocation density,  $\delta$ , measures the number of defects and vacancies in the crystal that is determined from the crystallite size using Scherrer's formula. From table 1, it was noted that there was an increase in dislocation density in basic medium. The highest  $\delta$  of 0.71  $\text{nm}^{-2}$  was recorded at pH 10, with the crystallite size of 11.84 nm. It is evident that the decrease in crystallite size causes an increase in the dislocation density.

Figures 3 to 5 showed plots of crystalline size, dislocation and lattice strain against pH of ZnO nanoparticles using Scherrer and Williamson-Hall (W-H) equations. In comparison, the values of the average crystallite size obtained for W-H analysis showed large variation; this variation was due to differences in averaging the particle distribution. The crystalline size recorded for W-H was between 28.32 and 75.52 nm and it is not in agreement with Scherrer's equation, with crystallite size of 11.84–24.82 nm. In this study, it implies that Scherrer's formula fitted well for the determination of grain size of ZnO. It was found that there were variation and increase in lattice strain in basic medium. Thus, the variation in strain could be due to the change in size and microstructure of the particles.

### 3.2. HRSEM analysis

The morphology of ZnO nanoparticles prepared through sol-gel method at pH 6, 8, 10 and 12 was investigated and presented in Plate 1. The as-synthesised ZnO nanoparticles were spherical shapes and particles were not in order in structures. Also, high agglomeration of the ZnO nanoparticles in the samples is clearly observed at lower pH. However, there was a decrease in the aggregation particles under the nucleation process on adding NaOH. It was found that the surface morphology significantly depends on this experimental parameter. The effect of pH on ZnO morphologies helps to explain the complexation of the  $\text{Zn}^{2+}$  ion, thus resulting in the complete reaction between the precursors leading to the formation of less agglomerated nanoparticles. The particle sizes of 26.10, 17.23, 14.90 and 16.38 nm for the pH of ZnO at 6, 8, 10 and 12 respectively were obtained. Figures 6 and 7 showed the EDX spectra of ZnO nanoparticles. The strong peaks of Zn and O were detected in the EDX spectra, which confirmed the formation of ZnO as the final product with C and Na as impurities. The spectrum of C is from the carbon support film on the grid. The weight and atomic percentage of these elemental compositions are presented in table 2. The as-synthesised ZnO nanoparticles have an atomic percentage of an approximately stoichiometric ratio of Zn (2): O (1) as shown in table 2.

### 3.3. FTIR analysis

Figure 8 shows the FTIR spectra of synthesised ZnO nanoparticles, pH at 6, 8, 10 and 12, calcined at 450 °C. At pH of 6 and 8, the wavenumber at 3300–3600  $\text{cm}^{-1}$  is assigned to the OH moiety which emanated from water and ethanol and is narrowed as the pH increases from 10 to 12. The bands appearing at 1456 and 1540  $\text{cm}^{-1}$  correspond to symmetric C=O and C–O stretching vibrations respectively while the peaks at 1630  $\text{cm}^{-1}$  are assigned to –COONa bond. The presence of peaks between 900 and 780  $\text{cm}^{-1}$  indicates that there are C–H groups emanating from the precursor used for ZnO synthesis. The ZnO moiety gives absorption bands of 513–710  $\text{cm}^{-1}$  at the fingerprint region, indicating the complete transformation of  $\text{Zn}(\text{OH})_2$  to ZnO. At pH of 6 and 12 when compared to pH of 8 and 10 in this study, peak shift between 1640 and 550  $\text{cm}^{-1}$  observed may be attributed to the change in average particle size distribution as a function of pH. However, the particle size

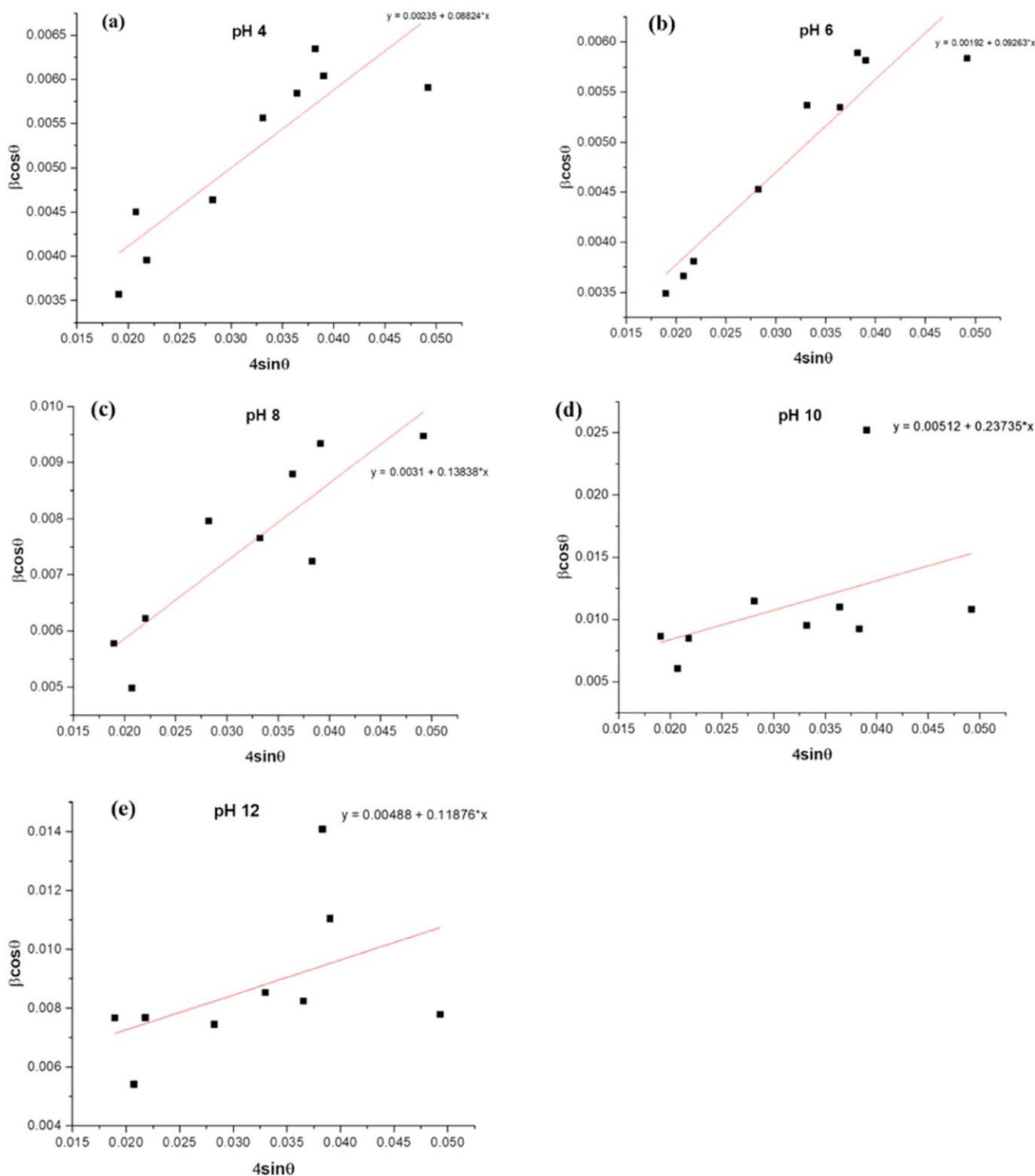


**Plate I.** HRSEM images of ZnO nanoparticles at pH (a) 6, (b) 8, (c) 10 and (d) 12 calcined at 450 °C.

caused a shift in wavelength. This observation is supported by XRD results (figure 9).

#### 4. Conclusion

ZnO nanoparticles at different pH were synthesised by sol-gel method using zinc acetate dihydrate as a precursor, sodium hydroxide as precipitating agent, and calcined at 450 °C to

examine the influence of different solution pH on the particle size, morphology and functional groups of the synthesised ZnO nanoparticles. The ZnO nanoparticles were characterised by XRD, HRSEM and FTIR. XRD analysis revealed the presence of zincite phase of ZnO. The XRD results also showed that average crystallite size decreased with the increase in pH at constant calcination temperature. From the HRSEM study, it was observed that ZnO nanoparticles



were spherically agglomerated in acidic medium but become less clustered in basic medium. The peak broadening was analysed by the Scherrer's formula and Williamson-Hall analysis. From the results, it was observed that the crystallite size using both methods decreased with an increase in pH. The crystallite size estimated from Scherrer's formula fitted well for the synthesised ZnO nanoparticles when compared to W-H analysis.

## Acknowledgments

The authors appreciate the financial support from the Tertiary Education Trust Fund (TETFund) of Nigeria under a grant number TETFUND/FUTMINNA/2017/01.

## References

- [1] Shaban M, Mohamed F and Abdallah S 2018 *Scientific Reports* **8** 3925
- [2] Ko T S, Yang S, Hsu H C, Chu C P, Lin H F, Liao S C, Lua T C, Kuo H C, Hsieh T W and Wang S C 2006 *Mater. Sci. Eng. B* **134** 54–8
- [3] Maryanti E, Damayanti D, Gustian I and Yudha S S 2014 *Materials Letters* **118** 96–8
- [4] Wallace R, Brown A P, Brydson R, Wegner K and Milne S J 2013 *J. Mater. Sci.* **48** 6393–403
- [5] Lang J, Wang J, Zhang Q, Li K, Han Q, Wei M, Sui Y, Wang D and Yang J 2016 *Ceramics Inter.* **42** 14175–81
- [6] Manjunath K et al 2014 *Mater. Res. Bulletin.* **57** 325–34
- [7] Jose A, Devi K R S, Pinheiro D and Narayana S L 2018 *J. Photochem. Photobiol. B* **187** 25–34
- [8] Parra M R and Haque F Z 2014 *J. Mater. Res. Technol.* **3** 363–9
- [9] Ashraf R, Riaz S, Hhaleeq-ur-Rehman M and Naseem S 2013 *The 2013 World Congress on Advances in Nano, Biomechanics, Robotics, and Energy Research (ANBRE 13)* (Korea: Seoul) (Aug. 25–28) 287–96
- [10] Bhardwaj R, Bharti A, Singh J P, Chae K H, Goyal N and Gautam S 2018 *Heliyon* **4** e00594
- [11] Manikandan B, Endo T, Kaneko S, Murali K R and John R 2018 *J. Mater. Sci. Mater. Electronics.* **29** 9474–85
- [12] Acosta-Humánez M, Montes-Vides L and Almanza-Montero O 2015 *Dyna* **83** 224–8
- [13] Mohan A C and Renjanadevi B 2016 *Procedia Technol.* **24** 761–6
- [14] Akkari M, Aranda P, Mayoral A, García-Hernández M, Amara A B H and Ruiz-Hitzky E 2017 *J. Hazardous Mater.* **340** 281–90
- [15] Kumar B R and Hymavathi B 2017 *J. Asian Ceramic Soc.* **5** 94–103